The ^{18}F-FDG PET Cingulate Island Sign and Comparison to ^{123}I-β-CIT SPECT for Diagnosis of Dementia with Lewy Bodies

Seok Ming Lim[1], Andrew Katsifis[2], Victor L. Villemagne[1,3], Rene Best[1], Gareth Jones[1], Michael Saling[4], Jennifer Bradshaw[4], John Merory[5], Michael Woodward[5], Malcolm Hopwood[6], and Christopher C. Rowe[1,3]

[1]Department of Nuclear Medicine and Centre for PET, Austin Health, Victoria, Australia; [2]Australian Nuclear Science and Technology Organization, Menai, New South Wales, Australia; [3]Department of Medicine, Austin Health, University of Melbourne, Victoria, Australia; [4]Department of Clinical Neuropsychology, Austin Health, University of Melbourne, Victoria, Australia; [5]Department of Aged Care, Austin Health, Victoria, Australia; and [6]Department of Psychiatry, Austin Health, Victoria, Australia

Neuroimaging is increasingly used to supplement the clinical diagnosis of dementia with Lewy bodies (DLB) by showing reduced occipital metabolism and perfusion and reduced striatal dopaminergic innervation. We aimed to optimize the interpretation of ^{18}F-FDG PET images for differentiating DLB from Alzheimer disease (AD) and to compare the results with dopamine transporter imaging using ^{123}I-β-carbomethoxy-3ß-(4-iodophenyl)-tropane (^{123}I-β-CIT) SPECT. **Methods:** Fourteen subjects with a clinical diagnosis of DLB and 10 with AD underwent both ^{18}F-FDG PET and ^{123}I-β-CIT SPECT. Four DLB and 1 AD diagnoses were subsequently confirmed at autopsy. Diagnostic accuracy was calculated for visual interpretation by 3 readers of standard 3-plane and stereotactic surface projection ^{18}F-FDG PET images, receiver-operating-characteristic analysis of regional ^{18}F-FDG uptake, and a cutoff value for the striatal-to-occipital binding ratio of β-CIT defined by receiver-operating-characteristic analysis. **Results:** Visual interpretation of 3-plane ^{18}F-FDG PET images had a sensitivity of 83% and specificity of 93% for DLB, slightly higher than the results with the stereotactic surface projection images. Regionally, hypometabolism in the lateral occipital cortex had the highest sensitivity (88%), but relative preservation of the mid or posterior cingulate gyrus (cingulate island sign) had the highest specificity (100%). Region-of-interest analysis revealed that occipital hypometabolism and relative preservation of the posterior cingulate both had a sensitivity of 77% and specificity of 80%. β-CIT achieved 100% accuracy and greater effect size than did ^{18}F-FDG PET (Cohen d = 4.1 vs. 1.9). **Conclusion:** Both ^{18}F-FDG PET and ^{123}I-β-CIT SPECT appear useful for the diagnosis of DLB, although the latter provides more robust results. The cingulate island sign may enhance the specificity of ^{18}F-FDG PET.

Key Words: dementia with Lewy bodies; emission tomography; ^{18}F-FDG; ^{123}I-β-CIT

J Nucl Med 2009; 50:1638–1645
DOI: 10.2967/jnumed.109.065870

Received May 6, 2009; revision accepted Jul. 10, 2009.
For correspondence or reprints contact: Christopher C. Rowe, Centre for PET, Austin Health, 145 Studley Rd., Heidelberg, Victoria 3084, Australia.
E-mail: christopher.rowe@austin.org.au

Dementia with Lewy bodies (DLB) is the second most common cause of neurodegenerative dementia after Alzheimer disease (AD), accounting for 15%−20% of cases examined at postmortem (*1*). Clinical diagnosis is less common, and there is a wide range of reported accuracy in diagnosis of DLB based on clinical criteria compared against neuropathologic findings, with specificity ranging from 30% to 100% and sensitivity from 20% to 90% (*2–7*). High specificity can be achieved in specialist centers, but diagnostic sensitivity remains limited.

DLB was originally defined as a clinicopathologic entity presenting with progressive cognitive decline interfering with normal social or occupational function, accompanied by a triad of core clinical features of fluctuating cognition, recurrent visual hallucinations, and spontaneous parkinsonism (*8*). Two core features allow a diagnosis of probable DLB and 1 of possible DLB. There has been a recent revision of these criteria, with the addition of suggestive features such as REM sleep behavior disorder, severe neuroleptic sensitivity, and loss of dopamine transporters (DATs) demonstrated by SPECT or PET (*9*).

Accurate and early diagnosis of DLB is important both for the clinical management of the disease and for the growth of the current body of knowledge, thus driving further research regarding its prognosis and treatment strategies. Most cases of DLB are erroneously mislabeled as AD, which can have major negative consequences for patients. For instance, neuroleptic drugs, commonly used for psychiatric symptoms and behavioral disturbances in dementia, can induce severe sensitivity reactions in DLB patients, exacerbating motor and mental instability and leading to a 2- to 3-fold increase in mortality (*10*). Cholinergic deficits appear greater in DLB, which might explain the greater improvement in visual, mood, and cognitive symptoms with cholinesterase inhibitors than usually seen in AD (*11*). A diagnosis of DLB would also prompt the clinician to consider additional DLB-specific

problems, such as extrapyramidal motor signs, gait and balance problems, autonomic dysfunction, and sleep disorders.

As such, there is growing interest in using neuroimaging to supplement the clinical diagnosis of DLB. Numerous studies have reported occipital hypoperfusion and hypometabolism in DLB patients, and parietotemporal reduction is common to both AD and DLB (*12–20*). The cingulate cortex in DLB, compared with in AD, appears to be relatively spared, but the clinical value of this finding has not been previously investigated (*21*). One study comparing autopsy results with PET findings found that glucose hypometabolism in the primary visual cortex distinguished DLB from AD with 90% sensitivity and 80% specificity (*13*).

Reduced nigrostriatal dopaminergic innervation also differentiates the DLB brain from AD and other causes of dementia. This pathologic feature can be studied via neuroimaging using radioligand binding to the DAT or vesicular monoamine transporter (*22–25*). SPECT with ^{123}I-β-carbomethoxy-3ß-(4-iodophenyl)tropane (^{123}I-β-CIT) examining the ratio of binding in the striatum to binding in the occipital cortex has been shown to reliably quantify DAT density (*26*). Recent studies using ^{123}I-*N*-3-fluoropropyl-2β-carbomethoxy-3β-(4-iodophenyl)tropane (^{123}I-FP-CIT) SPECT have reported sensitivities of 77%−100% and specificities of 83%−90% in differentiating clinically probable DLB from other causes of dementia (*16,27,28*). A recent study reported DAT SPECT to be more accurate than clinical diagnosis for DLB, with a sensitivity of 88% and specificity of 100%, compared with 75% and 42%, respectively, when evaluated against neuropathologic results in 20 patients with dementia (*29*).

In this study, we aimed to optimize visual and quantitative interpretation of ^{18}F-FDG PET images in differentiating DLB from AD and compare these results with DAT-based SPECT in the same patient cohort.

MATERIALS AND METHODS

Approval for the study was obtained from the Austin Health Ethics of Human Research Committee. Informed consent was obtained from both subjects and their spouses or caregivers after they were given a detailed description of the procedures involved. Subjects were recruited from the Austin Health Memory Disorders and Neurobehavioural Disorder Clinics and from affiliated neurologists and geriatricians. Subjects with a recent diagnosis of DLB or AD were asked by their treating specialist if they would like to participate in an imaging research project. Subjects who agreed to participate were then screened to ensure that the diagnostic criteria for probable DLB or probable AD were met before enrollment into the study. All subjects underwent standard clinical imaging (CT or MRI) and dementia screen blood tests; subjects who had a cortical stroke or multiple subcortical strokes or a potentially reversible cause of dementia or any other brain disorder or mental illness were excluded.

A total of 14 subjects who fulfilled the original DLB Consortium Consensus Criteria for probable DLB and 10 subjects who fulfilled the criteria of the National Institute of Neurological and Communicative Disorders and Stroke and the Alzheimer's Disease and Related Disorders Association for probable AD were studied (Table 1). The DLB and AD subjects all had progressive cognitive decline of less than 3 y duration and a mild to moderate score (1.0–1.5) on the Clinical Dementia Rating Scale.

AD subjects were significantly older, with a mean age of 79 y, compared with 72.5 y in the DLB cohort. The sex difference between DLB and AD groups reflects that found in the wider population, with more women in the AD group and a strong preponderance of men in the DLB cohort. Both groups were well matched in terms of cognitive function and functional severity of dementia; DLB subjects had more severe Parkinsonian features.

For comparison to normal-brain ^{18}F-FDG PET images, an existing database created at Austin Health consisting of 25 healthy, elderly subjects (mean age, 72 y) with normal brain MRI results, negative β-amyloid ^{11}C-Pittsburgh compound B PET scan results, and normal neuropsychology scores was used.

^{18}F-FDG PET Scans

Subjects were scanned on either a Siemens ECAT 951/31R PET camera (n = 18) (resolution, 6.5 mm in full width at half maximum [FWHM]) or a Phillips Allegro PET scanner (n = 6) (resolution, 5 mm in FWHM). Subjects fasted for 4 h before the injection of ^{18}F-FDG (250–300 MBq) and remained in a quiet, darkened room with their eyes open for 30 min. Acquisition started 30–45 min after injection. A postinjection transmission scan for attenuation correction was obtained. Acquisition time was 20 min per bed position, with 2 bed positions and 2-dimensional mode on the Siemens camera and 1 bed position and 3-dimensional (3D) mode on the Philips camera. Siemens images were reconstructed with an iterative filter (ordered-subset expectation maximization), and Philips images used a row-action maximum likelihood algorithm. Images were displayed on a workstation in the reader's preferred color scale.

Analysis

^{18}F-FDG PET scans were interpreted by 3 nuclear medicine physicians unaware of the clinical details. They were instructed to make a forced choice between DLB and AD.

Visual Interpretation. For each scan, the readers were asked to record a diagnosis of DLB or AD, the presence or absence of hypometabolism in the lateral occipital and medial occipital cortices, and whether relative preservation of the mid or posterior cingulate region was apparent. This finding is referred to as the cingulate island sign. Sensitivity and specificity for diagnosis of

TABLE 1. Patient Characteristics

Characteristic	Diagnosis		*P*
	DLB	AD	
n	14	10	
Age (y)	72. ± 5.9	79 ± 5.6	0.013
Sex	13 M, 1 F	2 M, 8 F	
MMSE	22.4 ± 4.6	23.4 ± 2.5	0.54
CDR	1.2 ± 0.55	0.97 ± 0.55	0.27
UPDRS	8.5 ± 2.7	1.4 ± 1.5	<0.0001

MMSE = Folstein Mini-Mental State Examination; CDR = Clinical Dementia Rating Scale; UPDRS = Unified Parkinson's Disease Rating Scale (5-item subscale; range, 0–20).

DLB were then calculated for each of the specified regions and the global impression. The mean results of the 3 readers were used for subsequent comparison of ^{18}F-FDG PET and β-CIT scans.

Regions of Interest (ROIs). Statistical parametric mapping (SPM99; Wellcome Department of Cognitive Neurology) was used to spatially normalize the ^{18}F-FDG PET scans, and ROIs were identified via the automated anatomic labeling (AAL) template (*30*). ROIs to be analyzed were the medial and lateral occipital cortices, precuneus, cuneus, posterior cingulum, and parietal cortex as shown in Figure 1. The mean voxel scores of each region were normalized to the cerebellar cortex and compared between the DLB and AD cohorts.

Results are expressed as mean and SD, and statistical comparison was performed through ANOVA. Cohen effect size (d) was calculated as the difference in the mean between the 2 cohorts divided by the pooled SD.

A receiver-operating-characteristic (ROC) curve was subsequently plotted for these cerebellar normalized ROIs to define the optimal cutoff value for distinguishing DLB from AD.

NEUROSTAT 3D-Stereotactic Surface Projection (3D-SSP). Individual ^{18}F-FDG PET scans were transformed into standard anatomic space via NEUROSTAT (Department of Radiology, University of Washington) and compared with the Austin ^{18}F-FDG PET reference database. The result was displayed with a color *z* score scale using the 3D-SSP software. The readers were asked to record the diagnosis of DLB or AD and detect the presence of hypometabolism (*z* score > 1.5) in the medial and lateral occipital cortices after viewing the 3D-SSP images.

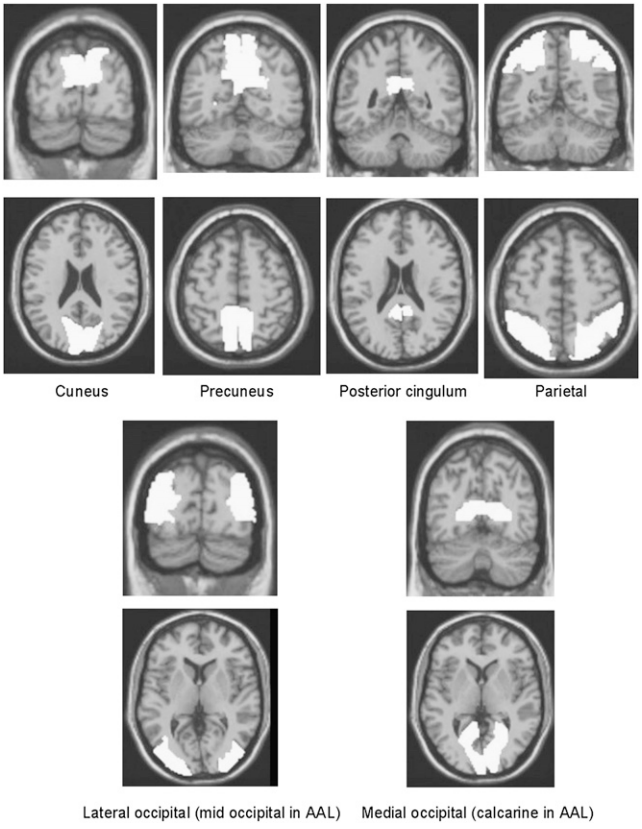

FIGURE 1. Axial and coronal images of ROIs as identified via AAL template for ^{18}F-FDG PET scans. Regions shown were normalized to cerebellar cortex and compared in DLB and AD cohorts.

^{123}I-β-CIT SPECT Scans

^{123}I-β-CIT was produced by the Radiopharmaceuticals Research Institute of the Australia Nuclear Science and Technology Organization and flown from Sydney to Melbourne for injection into the subjects the morning after production. ^{123}I-β-CIT was prepared by no-carrier-added ^{123}I-iododestannylation, followed by high-performance liquid chromatography purification (*31*). The radiochemical purity exceeded 99%, and the specific activity was greater than 185,000 GBq/mmol. All subjects underwent SPECT 22 h after the intravenous injection of ^{123}I-β-CIT (185–210 MBq) on a triple-head γ-camera (IRIX; Marconi Medical Systems) equipped with general-purpose collimators. Images were reconstructed with a Butterworth filter and attenuation-corrected with a Chang method attenuation coefficient of 0.12/cm. The resolution of the final image was 13 mm in FWHM.

Analysis

Three adjacent 5.4-mm-thick slices containing the highest uptake in the striatum were fused to construct a 16.2-mm-thick slice. Elliptic ROIs were placed over the right and left putamen (total area, 139.3 mm^2) and right and left caudate nucleus (total area, 116.6 mm^2) by an operator unaware of the clinical diagnosis. An irregular area measuring 1,545.5 mm^2 was drawn over the occipital cortex, which was used as the background sample because it does not contain DATs.

Specific striatal binding was expressed as V3″, the DAT binding parameter that is equivalent to k_3/k_4 and can be calculated on the basis of the above ROIs (*32*). V3″ was calculated as the ratio of the mean summation of the right and left caudate nucleus and putamen, compared with the occipital cortex (V3″ = [average striatum – occipital cortex]/occipital cortex).

Postmortem Findings

All study subjects were asked to consider postmortem brain donation to the Victorian Brain Bank Network. To date, postmortem histopathology results have been obtained on 5 study subjects: 4 DLB patients and 1 AD patient.

RESULTS

^{18}F-FDG PET Visual Interpretation

By visual inspection, ^{18}F-FDG PET had a mean sensitivity of 83% and specificity of 87% across the 3 readers in detecting DLB, with glucose hypometabolism in the lateral occipital area being most sensitive (Fig. 2). In comparison, the medial occipital area and cingulate island sign were found to be highly specific for DLB, with specificities of 97% and 100%, respectively, though sensitivities obtained ranged from 43% to 50% for the medial occipital and from 62% to 86% for the cingulate island sign. An example of the cingulate island sign is shown in Figure 3. Interobserver agreement for diagnosis of DLB or AD based on the whole ^{18}F-FDG PET image was high, with κ-measures of 0.56, 0.74, and 0.83 (mean, 0.71) when comparing one reader against another. NEUROSTAT-based analyses were slightly less accurate, with a mean sensitivity of 73% and specificity of 83% in detecting DLB.

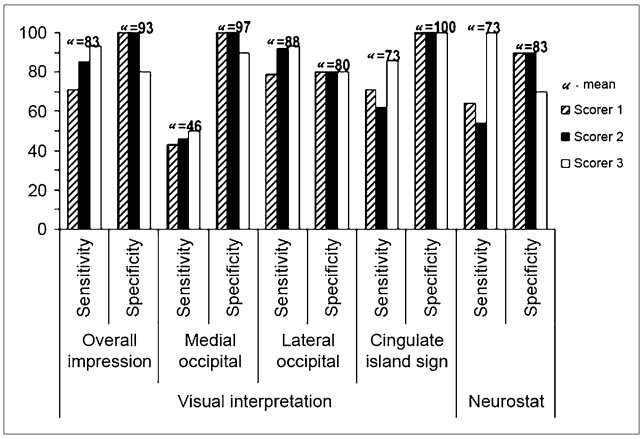

FIGURE 2. Sensitivity (%) and specificity (%) of ^{18}F-FDG PET for diagnosis of DLB via visual inspection by 3 readers. Mean results for 3 readers are expressed as μ numbers above each set of columns.

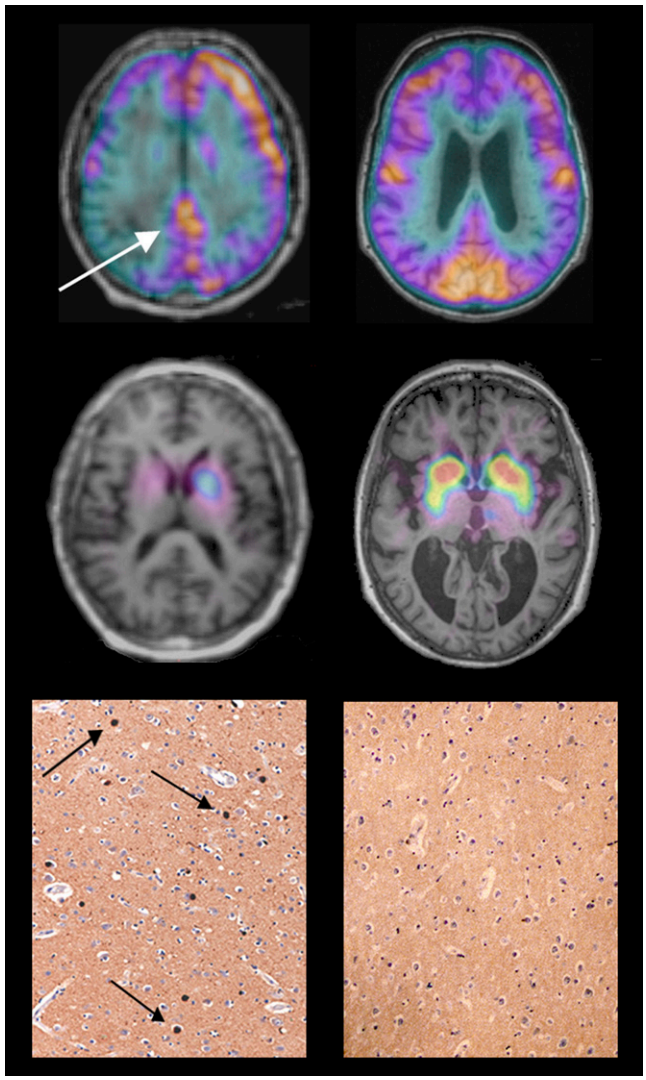

FIGURE 3. ^{18}F-FDG PET (top row) and β-CIT SPECT images (middle row) overlaid on MRI in patient with DLB (left column) and patient with AD (right column) who had diagnosis confirmed at autopsy. Immunohistochemical stain for α-synuclein demonstrates frequent Lewy bodies in DLB patient (black arrows) but none in AD patient. White arrow points to posterior cingulate cortex on ^{18}F-FDG PET study, demonstrating cingulate island sign of DLB.

AAL ROI Analysis

The DLB cohort, compared with AD subjects, had significantly lower metabolism across the medial occipital, lateral occipital, and parietal cortices. The ratio of the posterior cingulate gyrus to the adjacent precuneus and cuneus cortices was significantly higher in DLB subjects (Fig. 4).

Medial Occipital Cortex. DLB subjects, compared with AD and control subjects, showed hypometabolism in the medial occipital cortex. ROC analysis defined the optimal cutoff value for DLB against AD as 1.06. Using this value, we determined that the medial occipital ^{18}F-FDG uptake had an accuracy of 78% for diagnosis of DLB, with an effect size of 1.00.

Lateral Occipital Cortex. Both DLB and AD cohorts, compared with control subjects, were hypometabolic in the lateral occipital cortex. However, this feature was markedly more severe among DLB subjects, compared with AD subjects. The optimal cutoff point for DLB versus AD cohorts via ROC analysis was 0.91, with a diagnostic accuracy of 78% and an effect size of 1.72.

Parietal Region. DLB subjects, compared with control subjects, showed hypometabolism in the parietal region, and this was more severe than in the AD cohort. ROC analysis obtained a cutoff point of 0.88 in differentiating DLB from AD, with an accuracy of 78% and an effect size of 1.62.

Posterior Cingulate Region. Both groups, compared with control subjects, were hypometabolic in the posterior cingulate region. Contrary to the other regions analyzed, DLB subjects had a higher mean posterior cingulate ROI value than did AD subjects, though this was not significant.

Ratio of Posterior Cingulate to Surrounding Cortex. The ratio between the posterior cingulate and the surrounding precuneus and cuneus cortices was higher in DLB subjects than in AD subjects. The ratio of posterior cingulate to the sum of precuneus and cuneus distinguished DLB from AD with an accuracy of 78% and effect size of 1.94 via ROC analysis.

DAT Imaging

Visual inspection of DLB subjects, compared with AD subjects, showed global, often asymmetric reductions in striatal activity. Younger and less severely affected DLB subjects had reductions most marked in the putamen, with relative sparing of the caudate nucleus. In more severely

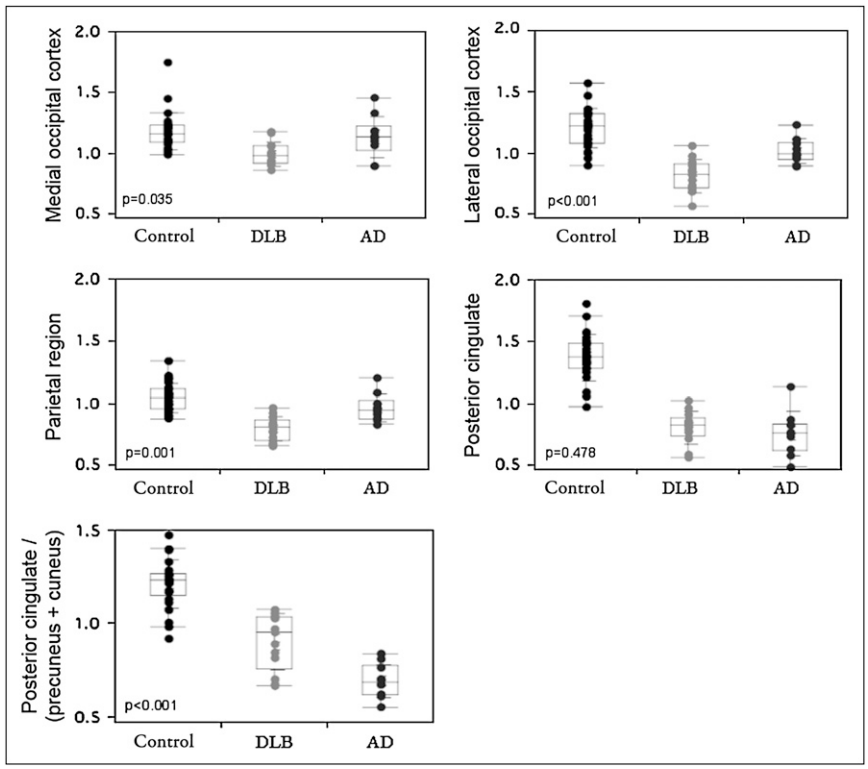

FIGURE 4. Individual results and box plot of median and interquartile range for ROIs shown in Figure 1. Results are expressed as mean voxel count in region divided by mean cerebellar cortex voxel count. *P* value is from ANOVA of 3 groups.

affected individuals, the reduction in DAT was more widespread throughout the striatum.

All DLB subjects, compared with the AD group, showed a marked reduction in the total ^{123}I-β-CIT uptake (Fig. 5). ROC analysis of DAT binding data revealed that a cutoff for V3″ of 4.0 produced 100% sensitivity and specificity for the diagnosis of DLB, with an effect size of 4.09. This value is equal to −1.5 SDs from the mean of the AD cohort.

Postmortem Findings

To date, 5 study subjects have undergone autopsy (Table 2). In all cases, neuropathologic diagnosis was concordant with the clinical diagnosis and that obtained via ^{18}F-FDG PET and β-CIT SPECT.

DISCUSSION

The diagnostic accuracy and effect size for the detection of DLB in a cohort of subjects with either DLB or AD were greater for DAT imaging with ^{123}I-β-CIT SPECT than for all ^{18}F-FDG PET measures of metabolism (Table 3). Although sample sizes were too small for this to be statistically significant, the difference in effect size—4.1 for β-CIT versus the best achieved with ^{18}F-FDG of 1.94—suggests that DAT imaging has a clinically meaningful diagnostic advantage.

However, ^{18}F-FDG PET also performed well, with best results achieved by global visual impression of the standard 3-plane slice display incorporating evaluation of hypometabolism in the lateral and medial occipital cortices and relative preservation of the mid or posterior cingulate cortex. The reading of NEUROSTAT 3D-SSP did not perform as well, probably because this display mode is not optimal for showing relative preservation in the posterior cingulate cortex. Although relative preservation of the cingulate cortex was previously reported in a quantitative analysis of ^{18}F-FDG PET in DLB (*21*), there has been no assessment of the clinical value of this observation for distinguishing DLB from AD. In our study, all 3 reviewers found this relative preservation, which we refer to as the cingulate island sign, to be 100% specific for DLB, with sensitivity ranging from 62% to 82%. The reduction in medial occipital metabolism was also highly specific for DLB but had poor sensitivity of 50% or less. Hypometabolism in the lateral occipital cortex was more sensitive but less specific, and this area is known to be involved in some cases of AD, in particular the posterior cortical atrophy variant.

The regional quantitation of ^{18}F-FDG images was less accurate than the visual reading of ^{18}F-FDG images (Table 3). Quantitation revealed that DLB subjects had more severe parietal and occipital hypometabolism than did the AD subjects, despite a similar degree of global cognitive impairment as assessed by the Mini-Mental State Examination and Clinical Dementia Rating Scale. This has been observed by others, and it has been proposed that the greater degree of hypometabolism in temporoparietooccipital association cortices reflects the worse visuospatial and visuoconstructive deficits in DLB patients, compared with

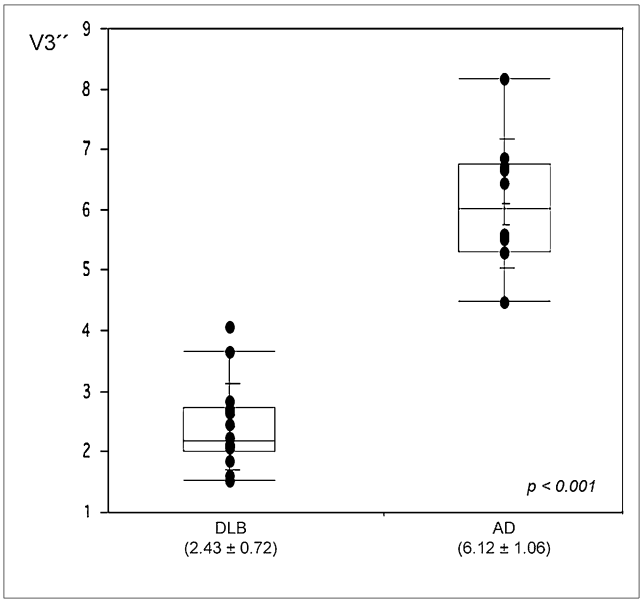

FIGURE 5. Box plot of median and interquartile range of DAT binding parameter obtained from ^{123}I-β-CIT scans. Results are calculated as V3″, ratio of mean striatum to occipital cortex. Values in brackets are mean ± SD.

AD patients (*20,21*). The reason for occipital hypometabolism among DLB patients is not clear. Some investigators have postulated that the changes in the occipital lobe might be linked to dopaminergic abnormalities in the visual pathway (*12*). Another hypothesis relates to the cholinergic system. Activity of choline acetyltransferase is lower in the temporoparietal and occipital neocortex in DLB, which might be secondary to neurodegenerative processes in the basal nucleus of Meynert, preferentially involving cholinergic neurons projecting to the occipital lobe. This selective deafferentation may contribute to the observed occipital hypometabolism (*33,34*). Supporting this possibility is the lack of occipital atrophy in MRI scans of DLB brains, suggesting that the occipital hypometabolism is not related to brain tissue loss but to disruption of intracortical connections (*35*).

Although, in a forced-choice design between DLB and AD subjects only, DAT imaging performed well, in the normal clinical environment, other causes for loss of nigrostriatal innervation must be considered and interpretation needs to be correlated with clinical assessment and structural imaging. Alternative nigrostriatal disorders such as Parkinson disease, multisystem atrophy, progressive supranuclear palsy, corticobasal degeneration, vascular parkinsonism with dementia, or frontotemporal dementia with parkinsonism can give rise to lowered DAT density. The density of DAT decreases with age at approximately 4% per decade in adulthood (*36*). In our study, this potential confounder was negated by the older age of the AD cohort, compared with the DLB group, but needs to be considered if a cutoff value has been derived from a cohort with a substantially different mean age.

A limitation of this study is the reliance on clinical diagnosis of DLB when the reported accuracy is highly variable. In this study, subjects met the strict criteria for probable DLB. Possible DLB cases were not included in an attempt to ensure high specificity of clinical diagnosis. Postmortem confirmation of diagnosis has been obtained in 5 subjects, and in these cases the findings were in agreement with the clinical diagnosis and imaging results. The remaining subjects have been followed clinically for several years with no change in diagnosis. Taken together, these factors suggest that our cohorts were well selected and the findings reported are valid.

Variation in DAT tracers, imaging equipment, acquisition protocols, and data processing means that our findings may not be directly applicable at other sites. However, in

TABLE 2. Neuropathologic and Imaging Findings of Subjects with Autopsy

Finding	Subject				
	1	2	3	4	5
Clinical diagnosis	DLB	DLB	DLB	AD	DLB
Amyloid-β plaques	+	—	++	+	++
Tau protein	—	—	+	+	—
Nigral neuronal loss	++	+++	++	—	+++
Cortical Lewy bodies	++	++	+++	—	+++
β-CIT V3″	2.7	2.14	2.09	6.72	3.67
^{18}F-FDG PET					
Lateral occipital cortex	0.74	0.68	0.80	0.85	0.81
Ratio of posterior cingulate/precuneus + cuneus	0.69	1.02	1.07	0.51	1.00
Visual ^{18}F-FDG PET					
Diagnosis	DLB	DLB	DLB	AD	DLB
Cingulate island sign	Y	Y	Y	N	Y
Final clinicopathologic diagnosis	DLB	DLB	DLB	AD	DLB

+ = mild; — = absent; ++ = moderate; +++ = severe; Y = yes; N = no.

TABLE 3. Sensitivity and Specificity of Various Modalities in Distinguishing DLB from AD

Modality	Cutoff	Sensitivity	Specificity	Effect size
Visual interpretation of ^{18}F-FDG PET	NA	83	93	NA
^{18}F-FDG PET NEUROSTAT	NA	73	83	NA
ROI analysis				
Medial occipital cortex	1.06	77	80	1.00
Lateral occipital cortex	0.91	77	80	1.72
Parietal region	0.88	77	80	1.62
Posterior cingulate/precuneus + cuneus	0.79	77	80	1.94
DAT V3″	4.5	100	100	4.09

NA = not applicable.

another study using ^{123}I-β-CIT SPECT, the mean striatal binding ratio (V3″) in AD (5.5 ± 1.1) and DLB (2.1 ± 0.4) were remarkably similar to our results (*37*). The current study should be repeated in a larger cohort of individuals representative of those presenting for diagnostic evaluation in clinical practice, to evaluate the clinical value of the findings that we have observed in patients without the full features of DLB. Such a study, using visual interpretation of ^{123}I-FP-CIT SPECT images and clinical diagnosis after 1 y of follow-up, has recently demonstrated useful diagnostic utility for DAT imaging across multiple centers (*38*).

CONCLUSION

This study supports the use of DAT imaging to distinguish subjects with DLB from those with AD. The interpretation of ^{18}F-FDG PET can be optimized by considering the lateral and medial occipital cortices and the cingulate island sign for differentiation of DLB from AD. Both approaches have high diagnostic accuracy, although DAT imaging appears to give more robust results.

ACKNOWLEDGMENTS

We acknowledge the Australian Institute of Nuclear Science and Engineering (AINSE) for funding the purchase of ^{123}I; ANSTO, and in particular Vahan Papazian and Tim Jackson, for the preparation of ^{123}I-β-CIT; and Guildford Pharmaceuticals (USA) for providing the β-CIT stannane for this work. Financial support was also provided by the Austin Hospital Medical Research Foundation.

REFERENCES

1. McKeith IG, Burn DJ, Ballart CG, et al. Dementia with Lewy bodies. *Semin Clin Neuropsychiatry.* 2003;8:46–57.
2. Luis CA, Barker WWW, Gajaraj K, et al. Sensitivity and specificity of three clinical criteria for dementia with Lewy bodies in an autopsy-verified sample. *Int J Geriatr Psychiatry.* 1999;14:526–533.
3. Litvan I, McIntyre A, Goetz CG, et al. Accuracy of the clinical diagnosis of Lewy body disease, Parkinson's disease and dementia with Lewy bodies. *Arch Neurol.* 1998;55:969–978.
4. McKeith IG, Ballard CG, Perry RH, et al. Predictive accuracy of clinical diagnostic criteria for dementia with Lewy bodies: a prospective neuropathological validation study [abstract]. *Neurology.* 1998;50(suppl 4):A181.
5. Papka M, Schiffer R, Rubia A. Diagnosing Lewy body disease: accuracy of clinical criteria in detecting Lewy body pathology [abstract]. *Neurobiol Aging.* 1998;19(4 suppl):203.
6. McShane RH, Esiri MM, Joachim C, et al. Prospective evaluation of diagnostic criteria for dementia with Lewy bodies [abstract]. *Neurobiol Aging.* 1998;19(4 suppl):204.
7. Mega MS, Masterman DL, Benson F, et al. Dementia with Lewy bodies: reliability and validity of clinical and pathologic criteria. *Neurology.* 1996;47:1403–1409.
8. McKeith IG, Galasko D, Kosaka K, et al. Consensus guidelines for the clinical and pathologic diagnosis of dementia with Lewy bodies (DLB): report of the consortium on DLB international workshop. *Neurology.* 1996;47:1113–1124.
9. McKeith IG, Dickson DW, Lowe J, et al. Diagnosis and management of dementia with Lewy bodies: third report of the DLB consortium. *Neurology.* 2005;65:1863–1872.
10. McKeith I, Fairbairn A, Perry R, Thompson P, Perry E. Neuroleptic sensitivity in patients with senile dementia of Lewy body type. *Br Med J (Clin Res Ed).* 1992;305:673–678.
11. Samuel W, Caligiuri M, Galasko D, et al. Better cognitive and psychopathologic response to donepezil in patients prospectively diagnosed as dementia with Lewy bodies: a preliminary study. *Int J Geriatr Psychiatry.* 2000;15:794–802.
12. Albin RL, Minoshima S, D'Amato CJ, et al. Fluoro-deoxyglucose positron emission tomography in diffuse Lewy body disease. *Neurology.* 1996;47:462–466.
13. Minoshima S, Foster NL, Sima AA, et al. Alzheimer's disease versus dementia with Lewy bodies: cerebral metabolic distinction with autopsy confirmation. *Ann Neurol.* 2001;50:358–365.
14. Ishii K, Yamaji S, Kitagaki H, et al. Regional cerebral blood flow difference between dementia with Lewy bodies and AD. *Neurology.* 1999;53:413–416.
15. Pasquier J, Michel BF, Brenot-Rossi I, et al. Value of ^{99m}Tc-ECD SPET for diagnosis of dementia with Lewy bodies. *Eur J Nucl Med Mol Imaging.* 2002;29:1342–1348.
16. Ceravolo R, Volterrani D, Gambaccini G, et al. Dopaminergic degeneration and perfusional impairment in Lewy body dementia and Alzheimer's disease. *Neurol Sci.* 2003;24:162–163.
17. Mirzaei S, Rodrigues M, Koehn H, et al. Metabolic impairment of brain metabolism in patients with Lewy body dementia. *Eur J Neurol.* 2003;10:573–575.
18. Gilman S, Koeppe R, Little R, et al. Differentiation of Alzheimer's disease from dementia with Lewy bodies utilising positron emission tomography with [^{18}F] fluorodeoxyglucose and neuropsychological testing. *Exp Neurol.* 2005;191(suppl 1):S95–S103.
19. Ishii K, Imamura T, Sasaki M, et al. Regional cerebral glucose metabolism in dementia with Lewy bodies and Alzheimer's disease. *Neurology.* 1998;51:125–130.
20. Higuchi M, Tashiro M, Arai H, et al. Glucose hypometabolism and neuropathological correlates in brains of dementia with Lewy bodies. *Exp Neurol.* 2000;162:247–256.
21. Imamura T, Ishii K, Sasaki M, et al. Regional cerebral glucose metabolism in dementia with Lewy bodies and Alzheimer's disease: a comparative study using positron emission tomography. *Neurosci Lett.* 1997;235:49–52.
22. Ceravolo R, Volterrani D, Gambaccini G, et al. Presynaptic nigrostriatal function in a group of Alzheimer's disease patients with parkinsonism: evidence from a dopamine transporter imaging study. *J Neural Transm.* 2004;111:1065–1073.
23. Koeppe RA, Gilman S, Joshi A, et al. ^{11}C-DTBZ and ^{18}F-FDG PET measures in differentiating dementias. *J Nucl Med.* 2005;46:936–944.
24. Bohnen NI, Frey KA. Imaging of cholinergic and monoaminergic neurochemical changes in neurodegenerative disorders. *Mol Imaging Biol.* 2007;9:243–257.

25. Gilman S, Koeppe RA, Little R, et al. Striatal monoamine terminals in Lewy body dementia and Alzheimer's disease. *Ann Neurol.* 2004;55:774–780.
26. Seibyl JP, Laruelle M, van Dyck C, et al. Reproducibility of iodine-123-β-CIT SPECT brain measurement of dopamine transporters. *J Nucl Med.* 1996;37: 222–228.
27. McKeith I, O'Brien J, Walker Z, et al. Sensitivity and specificity of dopamine transporter imaging with ^{123}I-FP-CIT SPECT in dementia with Lewy bodies: a phase III, multicentre study. *Lancet Neurol.* 2007;6:305–313.
28. Walker Z, Costa DC, Walker RWH, et al. Differentiation of dementia with Lewy bodies from Alzheimer's disease using a dopaminergic presynaptic ligand. *J Neurol Neurosurg Psychiatry.* 2002;73:134–140.
29. Walker Z, Jaros E, Walker RWH, et al. Dementia with Lewy bodies: a comparison of clinical diagnosis, FP-CIT single photon emission computer tomography imaging and autopsy. *J Neurol Neurosurg Psychiatry.* 2007;78:1176–1181.
30. Tzourio-Mazoyer N, Landeau B, Papathanassiou D, et al. Automated anatomical labelling of activations in SPM using a macroscopic anatomical parcellation of the MNI MRI single subject brain. *Neuroimage.* 2002;15: 273–289.
31. Katsifis A, Papazian V, Jackson, Loc'h C. A rapid and efficient preparation of [^{123}I]radiopharmaceuticals using a small HPLC (Rocket®) column. *Appl Radiat Isot.* 2005;64:27–31.
32. Laruelle M, Wallace E, Seibyl JP, et al. Graphical, kinetic, and equilibrium analyses of in vivo [^{123}I] beta-CIT binding to dopamine transporters in healthy human subjects. *J Cereb Blood Flow Metab.* 1994;14:982–994.
33. Forstl H, Burns A, Luthert P, Cairns N, Levy R. The Lewy-body variant of Alzheimer's disease: clinical and pathological findings. *Br J Psychiatry.* 1993; 162:385–392.
34. Perry EK, Haroutunian V, Davis KL, et al. Neocortical cholinergic activities differentiate Lewy body dementia from classical Alzheimer's disease. *Neuroreport.* 1994;5:747–749.
35. Ishii K, Soma T, Kono AK, et al. Comparison of regional brain volume and glucose metabolism between patients with mild dementia with Lewy bodies and those with mild Alzheimer's disease. *J Nucl Med.* 2007;48:704–711.
36. Lavalaye J, Booij J, Reneman L, et al. Effect of age and gender on dopamine transporter imaging with ^{123}I-FP-CIT SPET in healthy volunteers. *Eur J Nucl Med.* 2000;27:867–869.
37. Donnemiller E, Heilmann J, Wenning GK, et al. Brain perfusion scintigraphy with ^{99m}Tc HMPAO or ^{99m}Tc ECD and ^{123}I-β-CIT SPECT in dementia of the Alzheimer's type and diffuse Lewy body disease. *Eur J Nucl Med.* 1997;24:320–325.
38. O'Brien JT, McKeith IG, Walker Z, et al. Diagnostic accuracy of ^{123}I-FP-CIT in possible dementia with Lewy Bodies. *Br J Psychiatry.* 2009;194:34–39.